Proceedings Paper:

Deastra, P. orcid.org/0000-0002-1709-4686, Wagg, D. and Sims, N. (2020) Optimum design of a Tuned-Inerter-Hysteretic-Damper (TIHD) for building structures subject to earthquake base excitations. In: Papadrakakis, M., Fragiadakis, M. and Papadimitriou, C., (eds.) EURODYN 2020: Proceedings of the XI International Conference on Structural Dynamics. EURODYN 2020: XI International Conference on Structural Dynamics, 23-26 Nov 2020, Athens, Greece. European Association for Structural Dynamics (EASD) , pp. 1501-1509. ISBN 9786188507227

10.47964/1120.9121.18630

EURODYN 2020
XI International Conference on Structural Dynamics
M. Papadrakakis, M. Fragiadakis, C. Papadimitriou (eds.)
Athens, Greece, 22—24 June 2020

OPTIMUM DESIGN OF A TUNED-INERTER-HYSTERETIC-DAMPER (TIHD) FOR BUILDING STRUCTURES SUBJECTED TO EARTHQUAKE BASE EXCITATIONS

Predaricka Deastra[1], **David J. Wagg**, [2], **and Neil D. Sims**[2]

[1]PhD Student, Department of Mechanical Engineering, The University of Sheffield
Sir Frederick Mappin Building, Mappin Street, Sheffield S1 3JD
e-mail: pdeastra1@sheffield.ac.uk

[2] Professor, Department of Mechanical Engineering, The University of Sheffield
Sir Frederick Mappin Building, Mappin Street, Sheffield S1 3JD
e-mail: {david.wagg,n.sims}@sheffield.ac.uk

Keywords: Tuned-inerter-hysteretic-damper, hysteretic damping, seismic response, Self-adaptive Differential Evolution (SADE) algorithm, optimisation, time domain.

Abstract. *This paper discusses optimum design approaches for a novel tuned-inerter-hysteretic-damper (TIhD) which is a passive vibration suppression device for building structures subject to earthquake base excitations. The TIhD has a linear hysteretic damping element connected in series with an inerter. This device exploits the advantage of linear hysteretic damping which can reduce the structural response amplification at frequencies above resonance, due to the frequency dependent damping. In the present study, the effectiveness of this device in reducing seismic response of building structures is assessed and the optimum tuning of the device parameters is explored. In particular, eight different earthquakes are selected for a case study. The optimum parameters of the TIhD are obtained numerically by using the Self-Adaptive Differential Evolution (SADE) algorithm. The optimisation criterion is the minimum root-mean-square (RMS) value of the top-storey displacement response of the structure. The performance of this tuning configuration is then compared to that of a classically tuned device. The tuning performance is also compared across a range of simulated earthquakes, giving new insight into the challenges of optimising inerter designs that involve hysteretic damping.*

1 INTRODUCTION

In earthquake engineering practice, the use of inerters for suppressing structural vibration due to earthquakes has received a significant attention recently. An inerter is a two terminal mechanical device that generates forces proportional to the relative acceleration between its two terminals. In most studies, the inerter is combined with a spring and dashpot to form an inerter-based-damper (IBD). Several IBD concepts have been proposed in literature. Three of the most popular ones are the tuned-inerter-damper (TID), tuned-mass-damper-inerter (TMDI) and tuned-viscous-mass-damper (TVMD).

The TID was first introduced by Lazar et al. [1] in 2014. The layout of the TID is very similar to a classical tuned mass damper (TMD), but the mass m_d is replaced by an inerter element with inertance constant b_d. It has been shown to have a similar behavior with TMD. For example, the optimum tuning of the TID shows two equal peaks in the host structure frequency response assuming harmonic case. However, the presence of an inerter makes it possible to achieve a large mass ratio with a small physical mass. Furthermore it has been proven that the optimum location of the TID in a multi-storey building structure is on the base [1]. This is another benefit of the TID compared to the TMD, whose optimum location is on the top storey of a structure.

A study to enhance the TMD performance by employing an inerter led to a concept called tuned-mass-damper-inerter (TMDI) [2]. It is basically a TMD with an inerter connected in series. The TMDI can be considered as an ideal TID with the TMDI mass element m_d representing the physical mass of the inerter. When the inerter mass is zero ($m_d = 0$), the TMDI becomes a TID.

The first IBD introduced in the literature was the TVMD [3]. It consists of a parallel connected inerter and dashpot in series with a spring. A simple design method of the TVMD for MDOF structures can be found in [4]. The TVMD proposed in [4] combines a device called viscous-mass-damper (VMD) with a chevron bracing. The VMD is a combined inerter and dashpot in parallel. The inerter is given by a flywheel driven by a ball-screw mechanism and the dashpot is given by fluid flow. Another reaslisation of the TVMD can be found in [5], where a rack-and-pinion type of inerter was combined with an viscous damper in parallel. The spring element is given by a chevron bracing.

Recently, research on the IBD has been focused on three main areas: (1) The application and optimisation of IBD for different systems and condition, for examples see [6–8]; (2) Experimental validation, for examples see [9–11]; (3) studies of the IBD considering different layout or different type of inerter, stiffness and damping, for examples see [12–15]. From these three areas of research, one common discussion is about the IBD optimisation. Mostly, the optimisations of the IBD are based on the fixed-point theory (FPT) of Den Hartog [16]. However this is limited to the harmonic excitation case. For random and nonstationary signals such as earthquakes, often numerical approaches are used, for example see [8].

In this paper, an optimisation of a novel tuned-inerter-hysteretic-damper (TIhD) is discussed. The TIhD is the case when a material damper is connected in series with an inerter. In this case the material damper is represented by a linear hysteretic damping or complex stiffness. An extensive discussion about this concept has been discussed by the authors in a separate paper [17]. In the present work, a particular emphasis is given to the TIhD optimisation for building structures subject to earthquake base excitations. Specifically, a self-adaptive-differential-evolution (SADE) algorithm [18] is used to obtain the TIhD optimum parameters.

2 STRUCTURAL SYSTEM

To assess the structural performance with an optimized TIhD, a SDOF structure is selected as shown in Figure 1. Here m and k are the structural mass and stiffness respectively, and b_d is the

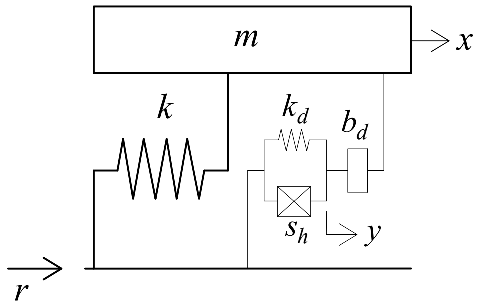

Figure 1: SDOF structure with a TIhD

TIhD inertance. For a numerical example in this paper, m and k are assumed to be 1tonne and 10kN/m. The hysteretic damping of the TIhD is represented by a complex stiffness $k_d(1 + j\eta)$, where $j = \sqrt{-1}$. k_d and s_h are the real and imaginary stiffness terms so that the loss factor is $\eta = s_h/k_d$. The structure is subjected to earthquake base displacement $r(t)$. The equation of motion of the structure is given by

$$\begin{cases} m\ddot{x}(t) + k(x(t) - r(t)) + b_d(\ddot{x}(t) - \ddot{y}(t)) = 0 \\ b_d(\ddot{x}(t) - \ddot{y}(t)) = k_d(1 + j\eta)(y(t) - r(t)) \end{cases} \tag{1}$$

where $x(t)$ and $y(t)$ are the displacement response of the lumped mass, m, and the TIhD displacement repectively.

It is important to note that the complex stiffness $k_d(1 + j\eta)$ is a noncausal model meaning physically it is not realisable. However, this model has been widely accepted in analysis [19] to accurately represent a class of nonlinear damping [20], as well as the phenomena of energy dissipation in a variety of materials such as rubber and viscoelastic polymers [21–24]. Due to its noncausality, it is common in practice to simplify the damping as a viscous damping via an equivalent viscous damping. This is in fact not accurate, especially at frequencies away from the resonance. Therefore a special time domain method is required to analyze such structure in the time domain as has been extensively discussed by the authors in [17].

3 OPTIMISATION PROCEDURE

In this paper, the time domain technique was adopted to optimize the TIhD parameters for a seismic application. Firstly, the TIhD was optimized based on an extended FPT adopted from Hu et al. [25] with an additional fine tuning procedure as discussed in [17]. For a given mass ratio, $\mu = \frac{b_d}{m} = 0.9$, the result is shown in Figure 2. In earthquake engineering practice this approach is not appropriate due to the broad band nature of the earthquakes, but it is often used for a preliminary design due to its simplicity.

Secondly, a SADE algorithm [18] was adopted to find the TIhD optimum parameters for some different earthquakes. The objective function is the minimum root-mean-square (RMS) value of the structural response $x(t)$. For one specific earthquake it is expressed by

$$\begin{gathered} b_{d_{min}} \leq b_d \leq b_{d_{max}}; k_{d_{min}} \leq k_d \leq k_{d_{max}}; \eta_{min} \leq \eta \leq \eta_{max} \\ min|\text{RMS}(x(t))| \end{gathered} \tag{2}$$

It is important to set a feasible limitation for b_d, k_d and η as shown in Eq.2 to reduce the computational cost. In this study, the limitations are $0.1 \leq b_d \leq 0.9; 0.1 \leq k_d \leq 10; 0.1 \leq \eta \leq 2$. Another important note is that the use of the SADE algorithm to obtain the RMS value of the structural response requires a time domain analysis. In this case, it has been made possible because of the time domain analysis proposed by the authors [17] for structures with linear hysteretic damping.

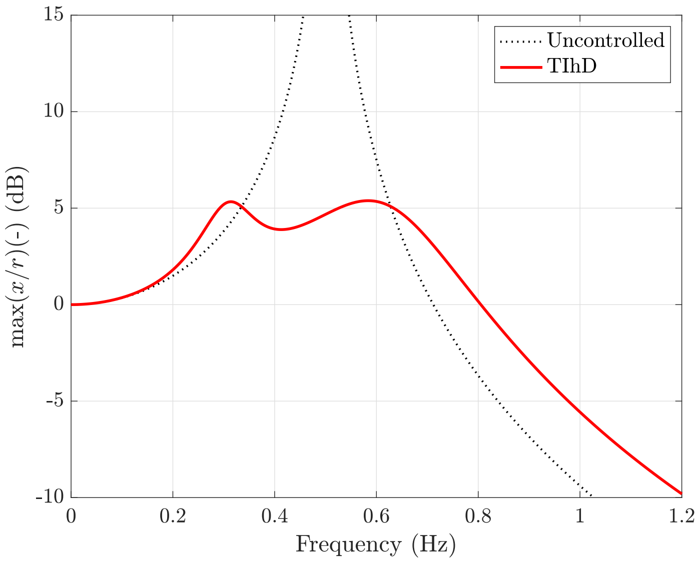

Figure 2: Maximum absolute displacement for $\mu = 0.9$, $k_d = 3.47$kN/m and $\eta = 1.26$

4 RESULTS AND DISCUSSION

In order to asses the effectiveness of the SADE algorithm against the FPT for minimizing a structural response subject to seismic excitations, eight different earthquakes were selected as shown in Figure 3.

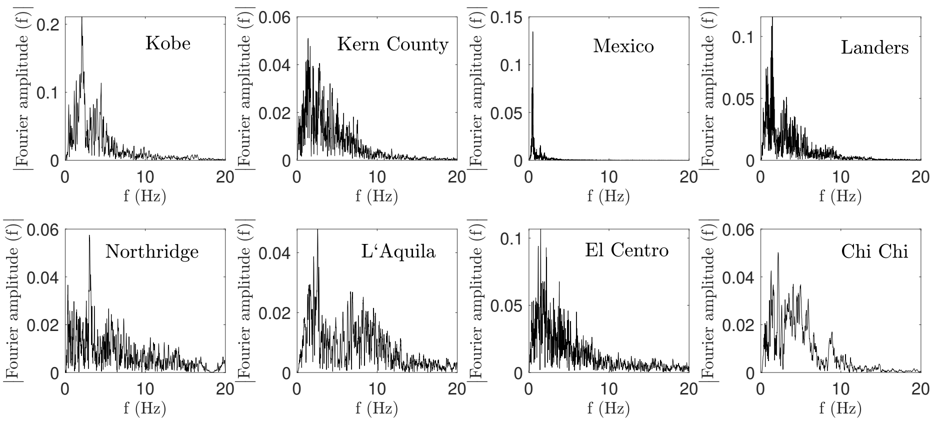

Figure 3: Fourier spectrum of the considered earthquakes ground motion

Figure 4 shows the RMS of the structural displacement response comparison between the optimised TIhD obtained by the FPT and by the SADE algorithm given by the Eq. 2. In this Figure, the RMS value of each earthquake is normalised against the RMS value from the FPT which is set to 100%. It is obvious that the SADE algorithm gives better reduction of the RMS value for all of the selected earthquakes. This is however not a practical solution because it leads to many inertance-stiffness-loss factor (ISL) configurations as shown in Table 1. For a realistic implementation, one configuration must be chosen, without prior knowledge of the specific earthquake excitation.

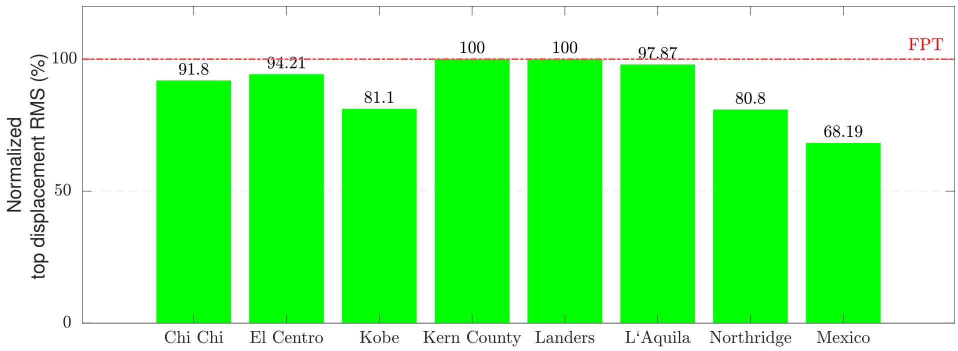

Figure 4: Normalised root mean square of the structural displacement response, SADE - Eq. 2

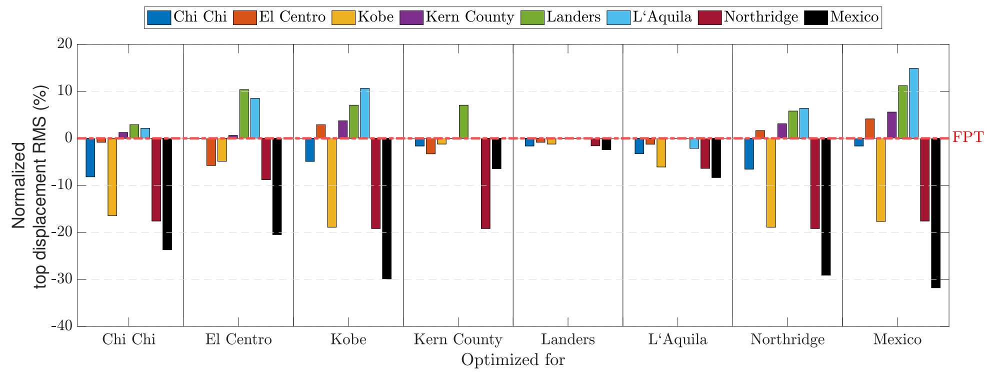

Figure 5: Cross-optimisation, SADE - Eq. 2

Figure 5 shows a cross-optimisation, meaning one configuration was selected from one particular earthquake to be used for simulation of other earthquake cases. For example, the first group of bars shows the structural response subjected to the eight considered earthquakes using one ISL configuration optimized for Chi Chi earthquake. The structural performance is being compared with the FPT which is set to 0%. Hence any negative values means a reduction on the structural response, on the other hand, any positive values means an amplification on the structural response relative to the FPT. For example, the group of bars for Landers implies that using one ISL configuration optimised for Landers earthquake for all other considered earthquakes makes the structural performance better than the one obtained via the FPT.

The group of bars for L'Aquila and Landers in Figure 5 in this case are the best result of this cross-optimisation since all other groups of bars show both positive and negative values. This simulation also implies that a correct formulation to chose or obtain the best ISL configuration is required. For this reason, a method that is based on the SADE algorithm was developed to find the best ISL configuration that gives minimum average RMS values of the structural performance subjected to a number of ground motions. It is expressed as

$$b_{d_{min}} \leq b_d \leq b_{d_{max}}; k_{d_{min}} \leq k_d \leq k_{d_{max}}; \eta_{min} \leq \eta \leq \eta_{max}$$
$$min\left|\frac{\sum_{i=1}^{n} \text{RMS}(x_i(t))}{n}\right| \tag{3}$$

where n is the number of considered earthquake input signals.

Figure 6 shows the structural performance comparison between the two approaches against the FPT. The second approach is (although not strictly better than the first approach) almost as good and clearly still superior than the FPT. It is in fact is more practical than the first approach because, as shown in Table 1, it has only one ISL configuration as in the case of the FPT. Two

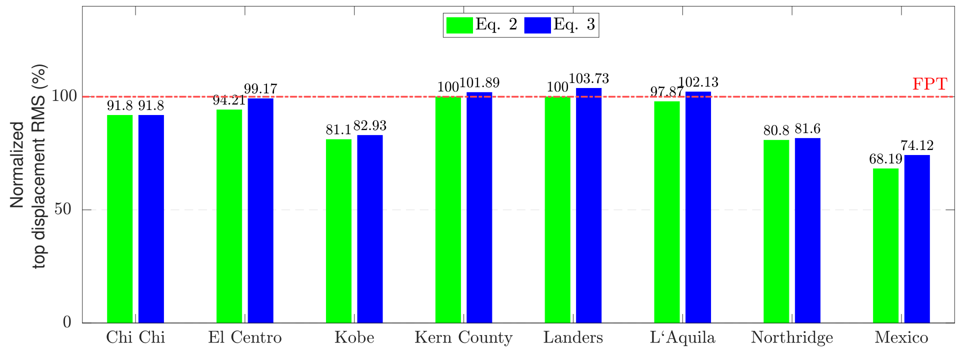

Figure 6: Normalised root mean square of the structural displacement response, SADE - Eq. 2 and 3

.

examples of the displacement response time history of the considered structure are given in Figure 7.

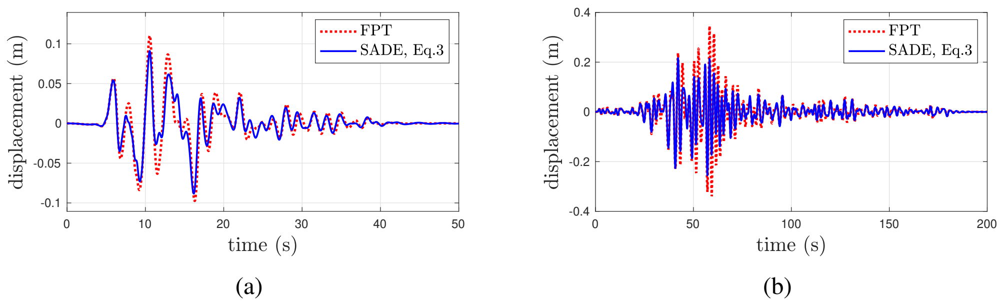

Figure 7: Examples of time history displacement response of the considered structure subjected to displacement ground motions (a) Kobe (b) Mexico

.

Table 1: TIhD optimum parameters

Earthquake	Fixed-point-theory (FPT)			SADE - Eq. 2			SADE - Eq. 3		
	b_d (Tonne)	k_d (kN/m)	η	b_d (Tonne)	k_d (kN/m)	η	b_d (Tonne)	k_d (kN/m)	η
Chi Chi	0.9	3.47	1.26	0.9	6.58	0.71	0.9	6.88	0.63
El-Centro				0.9	5.66	0.42			
Kobe				0.9	8.01	0.50			
Kern County				0.9	4.22	0.80			
Landers				0.9	3.71	1.14			
L'Aquila				0.9	4.30	1.06			
Northridge				0.9	7.68	0.54			
Mexico				0.9	8.16	0.39			

5 CONCLUSION

This paper presents the optimum design of the TIhD for long-period structures subjected to seismic ground motions. The optimisation method is based on the combined SADE algorithm and the time domain method for the TIhD to obtain the best ISL configuration of the TIhD.

There are two approaches presented in this study. The first approach is to find the minimum RMS value of the structural response for each of the considered earthquakes. Although the results show a superior benefit compared to the fixed point theory, it is however not practical because there is one ISL configuration obtained for one specific earthquake. As a result, there are many ISL configurations obtained depending on the number of the considered earthquake. The second approach is to find the best ISL configuration that gives minimum average RMS value of the structural response for all of the considered earthquakes. The second approach is considered to be a more practical solution and can be directly compared to the fixed point theory.

It has been shown that numerically optimised designs of TIhD can outperform those design using the classical fixed point theory. This is because the numerical method accommodates frequency independency, relying on a recently developed time-domain solution algorithm for hysteretic damping [17]. However this obviously requires a priori knowledge of the seismic excitation. Consequently further work should extend this approach to consider more formal earthquake design methodologies as part of the time-domain optimisation.

6 ACKNOWLEDGEMENT

PD would like to acknowledge the funding support from Indonesia Endowment Fund For Eduction (LPDP).

REFERENCES

[1] I.F. Lazar, S.A. Neild, D.J. Wagg, Using an inerter-based device for structural vibration suppression, *Earthquake Engineering & Structural Dynamics*, **43**,1129–1147, 2014.

[2] L. Marian, A. Giaralis, Optimal design of a novel tuned mass-damper-inerter (TMDI) passive vibration control configuration for stochastically support-excited structural systems,

Probabilistic Engineering Mechanics, **38**,156–164, 2014.

[3] K. Saito, Y. Sugimura, S. Nakaminami, H. Kida, N Inoue, *Vibration Tests of 1-story Response Control System Using Inertial Mass and Optimized Soft Spring and Viscous Element. Proceedings of the 14th World Conference on Earthquake Engineering*, 2008.

[4] K. Ikago, Y. Sugimura, K. Saito, N Inoue, *Simple Design Method for a Tuned Viscous Mass Damper Seismic Control System. Proceedings of the 15th World Conference on Earthquake Engineering*, 2012.

[5] R.M. Hessabi, O. Mercan, Investigations of the application of gyro-mass dampers with various types of supplemental dampers for vibration control of building structures, *Engineering Structures*, **126**,174–186, 2016.

[6] A. Di Matteo, C. Masnata, A. Pirrotta, Simplified analytical solution for the optimal design of Tuned Mass Damper Inerter for base isolated structures, *Mechanical Systems and Signal Processing*, **134**,106337, 2019.

[7] Z Zhao, Q. Chen, R. Zhang, C. Pan, Y. Jiang, Optimal design of an inerter isolation system considering the soil condition, *Engineering Structures*, **196**,109324, 2019.

[8] D. De Domenico, P. Deastra, G. Ricciardi, N.D. Sims, D.J. Wagg, Novel fluid inerter based tuned mass dampers for optimised structural control of base-isolated buildings, *Journal of the Franklin Institute*, **356**,7626–7649, 2019.

[9] X. Liu, B. Titurus, J.Z. Jiang, Generalisable model development for fluid-inerter integrated damping devices, *Mechanism and Machine Theory*, **137**,1–22, 2019.

[10] E.D.A John, D.J. Wagg, Design and testing of a frictionless mechanical inerter device using living-hinges, *Journal of the Franklin Institute*, **356**,7650–7668, 2019.

[11] C. Málaga-Chuquitaype, C. Menendez-Vicente, R. Thiers-Moggia, Experimental and numerical assessment of the seismic response of steel structures with clutched inerters, *Soil Dynamics and Earthquake Engineering*, **121**,200–211, 2019.

[12] S. Zhou, C. Jean-Mistral, S. Chesne, Influence of inerters on the vibration control effect of series double tuned mass dampers: Two layouts and analytical study, *Structural Control & Health Monitoring*, **26**,e2414, 2019.

[13] A. Javidialesaadi, N.E. Wierschem, Optimal design of rotational inertial double tuned mass dampers under random excitation, *Engineering Structures*, **165**,412-421, 2018.

[14] X. Shi, S. Zhu, A comparative study of vibration isolation performance using negative stiffness and inerter dampers, *Journal of the Franklin Institute*, **356**,7922-7946, 2019.

[15] Z. Zhao, R. Zhang, Y. Jiang, C. Pan, A tuned liquid inerter system for vibration control, *International Journal of Mechanical Sciences*, **164**,105171, 2019.

[16] J.P. Den Hartog, (1956) Mechanical Vibrations (4th edition), Dover: New York.

[17] P. Deastra, D.J. Wagg, N.D. Sims, M. Akbar, Tuned-inerter-dampers with linear hysteretic damping. (*under review*).

[18] A.K. Qin, P.N. Suganthan, *Self-adaptive Differential Evolution Algorithm for Numerical Optimization, 2005 IEEE Congress on Evolutionary Computation,* **2**, 1785–1791, 2005.

[19] C.F. Beards, (1996) Structural Vibration: Analysis and Damping, Halsted Press: New York-Toronto.

[20] J.A. Inaudi, M. Kelly, A friction mass damper for vibration control, *Report No. UCB/EERC-92/18, Earthquake Engineering Research Center, University of California at Berkeley, 1992*.

[21] R.M. Joseph, A.B. Kirsten, C.P. Scott, *Complex stiffness measurement of vibration damped structural elements. Proceedings of the International Modal Analysis Conference, Vol. 1, p. 391-397.*, 2000.

[22] D.R. Mohan, G. Scott, G. Dave, *Measurement of dynamic parameters of automotive exhaust hangers. SAE Technical Papers, Noise and Vibration Conference and Exposition, Vol. 1, p. 1-8.*, 2001.

[23] B. Bloss, D.R. Mohan, Measurement of damping in structures by the power input method, *Experimental Techniques*, **26**, Issue 3, 30–32, 2002.

[24] E.O. Lu, M.R. Zaidi, Dynamic stiffness and loss factor measurement of engine rubber mount by impact test, *Materials and Design*, **32**, 1880–1887, 2011.

[25] Y. Hu, M.Z.Q Chen, Z. Shu, L. Huang, Analysis and optimisation for inerter-based isolators via fixed-point theory and algebraic solution, *Journal of Sound and Vibration*, **346**,17–36, 2015.